Ticks and Tick-borne Diseases 15 (2024) 102304

Contents lists available at ScienceDirect

Ticks and Tick-borne Diseases

journal homepage: www.elsevier.com/locate/ttbdis

Original article

A longitudinal transcriptomic analysis of *Rhipicephalus microplus* midgut upon feeding

Stephen Lu [a], Jéssica Waldman [b], Luís Fernando Parizi [b], Itabajara da Silva Vaz Junior [b,c], Lucas Tirloni [d,*]

[a] Vector Biology Section, Laboratory of Malaria and Vector Research, National Institute of Allergy and Infectious Diseases, Bethesda, MD, United States
[b] Centro de Biotecnologia, Universidade and Faculdade de Veterinária, Universidade Federal do Rio Grande do Sul (UFRGS), RS, Brazil
[c] Instituto Nacional de Ciência e Tecnologia - Entomologia Molecular, Rio de Janeiro, RJ, Brazil
[d] Tick-Pathogen Transmission Unit, Laboratory of Bacteriology, National Institute of Allergy and Infectious Diseases, Hamilton, MT, United States

ARTICLE INFO

Keywords:
Ticks
Blood meal digestion
Midgut
RNA-sequencing

ABSTRACT

Rhipicephalus microplus, a highly host-specific tick that primarily feeds on cattle, posing a significant threat to livestock production. The investigation of tick physiology is crucial for identifying potential targets in tick control. Of particular interest adult female ticks undergo a significant expansion of the midgut during feeding, leading to an over 100-fold increase in body weight. Beyond the functions of storing and digesting blood meals, the tick midgut plays a crucial role in acquiring and transmitting pathogens. However, our understanding of tick midgut physiology remains limited. In this study we conducted a comprehensive longitudinal transcriptome analysis of the midgut from adult female *R. microplus* ticks collected at various feeding stages, providing an overview of the transcriptional modulation in this organ as feeding progress. By employing a *de novo* assembly approach followed by coding-sequences (CDS) extraction, 60,599 potential CDS were identified. In preparation for functional annotation and differential expression analysis, transcripts that showed an average transcript per million (TPM) ≥ 3 in at least one of the biological conditions were extracted. This selection process resulted in a total of 10,994 CDS, which were categorized into 24 functional classes. Notably, our differential expression analysis revealed three main transcriptional profiles. In the first one, representing the slow-feeding stage, the most abundant functional classes were the "protein synthesis" and "secreted" groups, reflecting the highly active state of the tick midgut. The second profile partially accounts for the rapid-feeding stage, in which a high number of differentially expressed transcripts was observed. Lastly, the third transcriptional profile represents post-detached ticks. Notably the highest number of modulated transcripts was observed up to 48 h post-detachment (hpd), however no major differences was observed up to 168 hpd. Overall, the data presented here offers a temporal insight into tick midgut physiology, contributing to the identification of potential targets for the development of anti-tick control strategies.

1. Introduction

The behavior of blood-feeding has evolved independently multiple times within the Arthropoda phylum (Mans, 2011). In the case of the Acari subgroup, it is proposed that hematophagy has a monophyletic origin (Mans and Francischetti, 2016). Specifically, in female ixodid ticks, blood feeding is traditionally subdivided into three main phases: the preparatory feeding, in which the tick attaches to the host's skin and establishes the feeding lesion; the slow-feeding which spans multiple days; and the rapid-feeding phase, which takes place in the last 12 to 24 h of feeding (Franta et al., 2010). During the last feeding phase, the mated female ingest vast amounts of blood increasing its body weight over 100-fold (Sonenshine, 2013).

As feeding progresses, the tick midgut undergoes dramatic morphological alterations. Initially, the midgut of unfed adult females is typically described as a "small tube-like extension" with an almost empty lumen primarily composed of a monolayer of undifferentiated cells (UC) (Agyei and Runham, 1995). However, as the tick begins to feed, the lumen gradually expands, and the UCs differentiate into digestive cells (DC) (Sonenshine, 2013) (Agyei et al., 1991). These

* Corresponding author.
E-mail address: lucas.tirloni@nih.gov (L. Tirloni).

https://doi.org/10.1016/j.ttbdis.2023.102304
Received 16 October 2023; Received in revised form 20 December 2023; Accepted 21 December 2023
Available online 30 December 2023

specialized cells possess the ability to specifically recognize and internalize hemoglobin (Lara et al., 2005). In contrast to many other blood-feeding arthropods, ticks process hemoglobin intracellularly, utilizing cysteine and aspartic peptidases (Horn et al., 2009). In fully fed ticks, the digestive cells are fully stretched and exhibit multiple cytoplasmatic vesicles. In some instances, these cells are observed "floating" in the midgut lumen (Franta et al., 2010). Moreover, the tick midgut also plays a pivotal role in the tick's vector competency. When a pathogen enters the tick midgut, a series of specific interactions between pathogen and tick molecules must occur to ensure pathogen survival and proliferation (Maeda et al., 2017; Rachinsky et al., 2008; Pal et al., 2004; Yang et al., 2021).

Rhipicephalus microplus is an ixodid tick species known for its high host specificity to bovines. This tick species spends its entire parasitic life cycle attached to a single host, leading to significant losses in livestock production (Lew-Tabor and Valle, 2016; Grisi et al., 2014). Currently, tick control relies mainly on acaricides, which has potential drawbacks such as the selection of resistant tick populations (Becker et al., 2019; Li et al., 2007). This highlights the need for cost-efficient and environmentally friendly alternative control strategies. Notably, in the case of *R. microplus*, immunological control has been shown to be a viable alternative. Vaccination of cattle against a tick midgut protein (Bm86) resulted in an effective anti-tick response (Rand et al., 1989; Willadsen et al., 1989). However, it is essential to emphasize that the level of protection achieved can vary depending on the specific tick population (Andreotti, 2006). This observation underscores the importance of identifying antigens that can induce an effective protection against various tick populations or species, a challenge that remains a bottleneck in the development of anti-tick vaccines (Rego et al., 2019).

Therefore, to advance our understanding of tick midgut physiology, which may lead to the identification of potential targets for the development of new methods for tick control, we conducted an in-depth temporal transcriptome analysis of the *R. microplus* midgut. This analysis covered sequential feeding times, spanning both the slow- and rapid-feeding, as well as multiple time points post-detachment. Our study not only showcases the extensive repertoire of midgut transcripts but also offers valuable insights into the temporal organization and alterations in the expression profiles of key metabolic pathways within the midgut as feeding progresses.

2. Materials and methods

2.1. Ethics statement

The research was conducted in strict adherence to ethical and methodological guidelines, in accordance with the International and National Directives and Norms by the Animal Experimentation Ethics Committee of Universidade Federal do Rio Grande do Sul, Brazil (UFRGS), under project number 27,559.

2.2. Tick rearing and midgut dissection

Rhipicephalus microplus ticks (Porto Alegre strain) were obtained from cattle housed in insulated boxes at UFRGS. Calves were infested with larvae, and after 21 days, partially engorged and fully engorged adult female ticks were collected (Reck et al., 2009). Organ dissection involved manually removing partially engorged females from the cattle, weighing approximately 38.9 ± 4.48 mg (G1), 60.8 ± 10.1 mg (G2), 94.7 ± 9.0 mg (G3), and 192.9 ± 12.4 mg (G4). Fully engorged females were dissected at 0, 24, 48, 72, 120, 144, and 168 h post detachment (hpd) from the host. The midguts were separated using fine-tipped forceps and then washed with diethyl pyrocarbonate-phosphate-buffered saline (DEPC-PBS) at pH 7.2. These dissected tissues were washed with cold DEPC-PBS and added in RNAlater solution, stored at 4 °C for 24 h, and subsequently stored at −70 °C until RNA extraction.

2.3. Library preparation, sequencing, and data analysis

The total RNA was isolated using the AllPrep DNA/RNA/Protein Mini Kit (QIAGEN), following the manufacturer's instructions. Illumina libraries were prepared using the NEBNextUltraTM II (Directional) RNA with polyA selection, and library sequencing was conducted on an Illumina Novaseq 6000 DNA sequencer. The quality of the raw reads was assessed using the FastQC tool (https://www.bioinformatics.babraham.ac.uk/projects/fastqc/). Low-quality sequences with a Phred quality score (Q) below 20 and the Illumina adaptors were removed using TrimGalore (https://github.com/FelixKrueger/TrimGalore). Subsequently, reads were merged and *de novo* assembled using Trinity (2.9.0) (Grabherr et al., 2011), in single-stranded F mode, and ABySS (2.3.1) (Simpson et al., 2009) with k values ranging from 25 to 95, with increments of 10. The final assemblies were merged, and sequences sharing at least 95 % identity were consolidate using the CD-HIT tool (Fu et al., 2012). The DNA coding sequences (CDS) with an open reading frame (ORF) of at least 150 nucleotides were extracted based on BLASTp results from several databases, including a subset of the non-redundant protein database, the transcriptome shotgun assembly (TSA), and Refseq-invertebrate. The CDS were extracted if they covered at least 70 % of a matching protein. Additionally, all ORFs starting with a methionine and with a length of at least 40 amino acids were subjected to the SignalP tool (V3.0). Sequences with a putative signal peptide were mapped to the ORFs, and the most 5′ methionine was selected as the starting point of the transcript (Bendtsen et al., 2004). Relative quantification of each putative CDS was estimated using the transcript per million (TPM) parameter by mapping the trimmed Illumina reads to the final list of CDS using RSEM (Li and Dewey, 2011). Functional annotation of the selected CDS was carried out using an *in-house* program that scanned a vocabulary of approximately 400 words and their order of appearance in the protein matches obtained from BLASTp/RPS-BLAST against various databases, including Transcriptome Shotgun Assembly (TSA), a subset from the Non-Redundant (NR), Refseq-invertebrate, Refseq-vertebrate, Refseq-protozoa, UNIPROT, CDD, SMART, MEROPS, and PFAM. This annotation process included percent identities and coverage information (Karim et al., 2011). The final annotated CDS are available for download as a hyperlinked Excel file (Supplementary file 1). Transcriptome completeness was evaluated using the Benchmarking Universal Single-Copy Orthologs utilizing the Arachnida database as reference (Simao et al., 2015).

2.4. Statistical analysis

Differential expression analysis was conducted using the *edgeR* package (Robinson et al., 2010) in R (Team, 2020). Statistical significance was considered when the Log2 (fold change) was greater than 2 or lesser than –2, and the false discovery rate (FDR) was less than 0.05. The heatmap plot was generated using the *pheatmap* package, using the TPM values represented as percentages, while the volcano plots were generated using the *ggplot2* package in R. Unsupervised clustering of the filtered CDS was performed using the Expander tool with the CLICK method (Shamir et al., 2005), utilizing the number of mapped reads of each CDS.

3. Results and discussion

3.1. Overview of the longitudinal transcriptome of R. microplus midgut

After excluding the Illumina adapters and low-quality sequences ($Q<20$), we obtained a total of 1125,836,934 high-quality reads from midgut samples collected from *R. microplus* ticks at various stages during the blood feeding and post detachment (Fig. 1A). Utilizing a *de novo* assembly approach that combined results from Trinity and ABySS, followed by our CDS extraction pipeline, enabled the identification of 60,599 potential CDS. To assess the relative abundance of each CDS, we

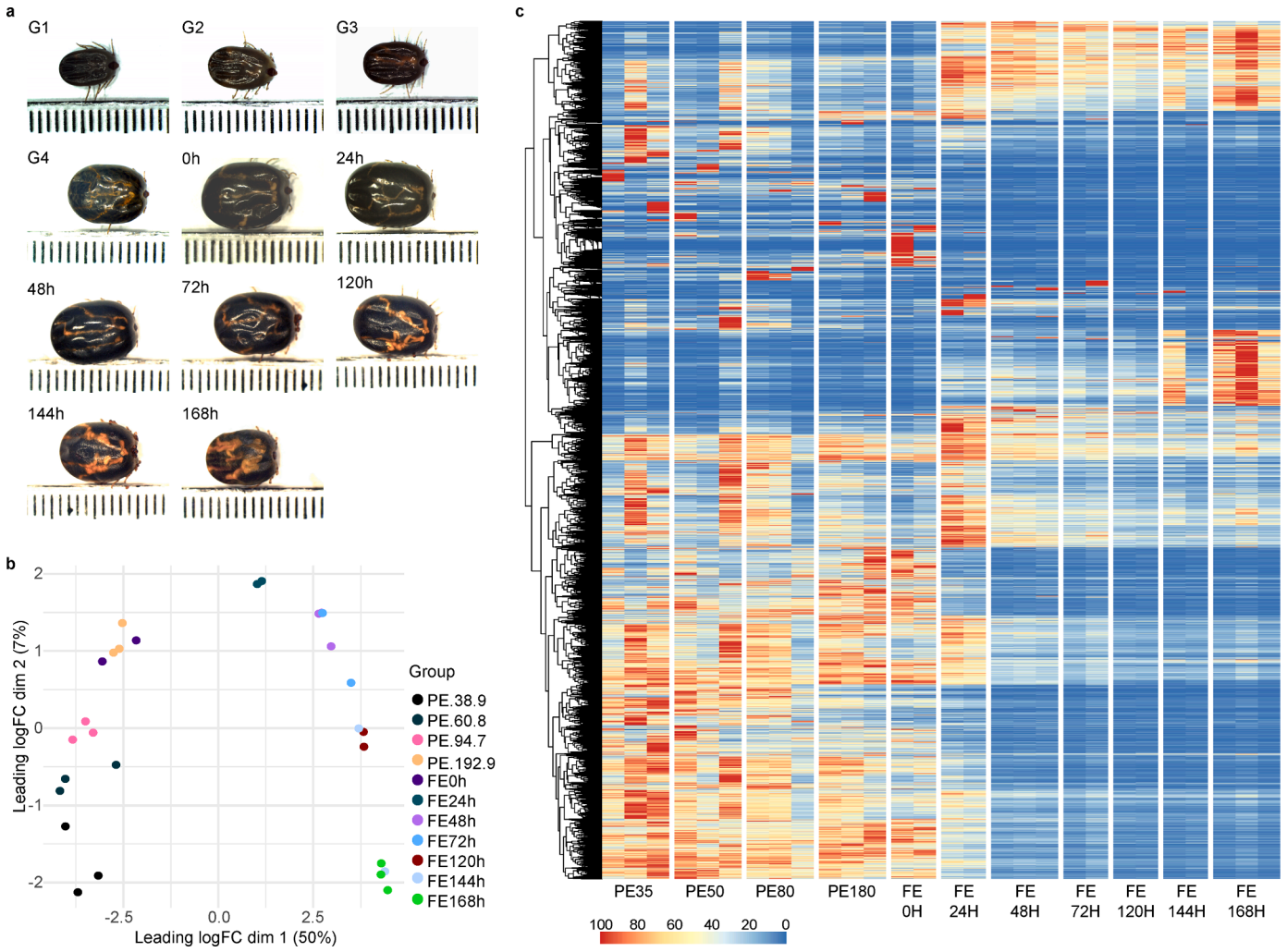

Fig. 1. Overview of the transcriptome profile of *Rhipicephalus microplus* midgut at different feeding stages. (A): Representative images of the collected ticks by their average weight or hours post-detachment. Each dot represents 1 mm. (B): Multidimensional plot of the transcripts with transcript per million (TPM) $\geq$ 3 in at least one of the biological groups. (C): Heatmap plot using the normalized TPM values of each transcript. Each column represents a biological replicate. G1 – G4 indicates partially fed ticks that were collected and grouped based on their average weight; (G1) 38.9 $\pm$ 4.48 mg, (G2) 60.8 $\pm$ 10.1 mg, (G3) 94.7 $\pm$ 9.0 mg and (G4) 192.9 $\pm$ 12.4 mg. While 0 h – 168 h represents ticks collected at different time points after their natural detachment from its host.

used the RSEM tool to map the trimmed Illumina reads to the extracted CDS. It is important to note that all biological replicates of each biological condition exhibited similar mapping rates (Supplementary Table 1) and demonstrated coherent clustering within their respective biological groups (Fig. 1B). These results collectively underscore the absence of significant bias in our sample set. Furthermore, employing the Benchmark Universal Single Copy-Orthologue (BUSCO) analysis, using the Arachnida database as reference, revealed a completeness assessment of 57 % (49.0 % single and 7.1 % duplicate), 2.4 % fragmented and 40.6 % missing. In preparation for functional annotation and differential expression analysis, we extracted transcripts that exhibited an average TPM $\geq$ 3 in at least one of the biological conditions. This selection process yielded a total of 10,994 CDS (Supplementary file 1).

Prior investigations of tick midgut contents have provided limited insights into the evolving dynamics within this organ during feeding, often focusing on isolated time points (J. Perner et al., 2016; Landulfo et al., 2017; Schwarz et al., 2014). More recently, our group conducted a longitudinal transcriptome study of the *Ixodes scapularis* midgut, covering different phases during the feeding process (Lu et al., 2023). This analysis unveiled four main transcriptional profiles, characterizing the unfed, slow-feeding, rapid-feeding, and early post-detachment stages. However, in the current dataset, the dimensional analysis (Fig. 1B) indicates the presence of only two prominent transcriptional profiles. Specifically, the X-axis accounts for 50 % of the variance, while the Y-axis explains only 7 %, effectively categorizing our samples into two distinct groups. The first group comprises pre-detached ticks, regardless of their weight, and recently detached fully fed ticks (0 h). The second group consists of ticks that have surpassed 24-hpd. Similarly, the heatmap plot of the normalized TPM values for each transcript (Fig. 1C) reveals a similar dichotomous pattern. Transcripts that are abundant in the early feeding stages become nearly absent in the later stages, and vice versa. It is important to note that transcript levels do not always correlate well with actual protein content in a given sample, and further proteomics studies are necessary to validate the contents of tick midguts.

To gain further insight into *R. microplus* midgut physiology, we classified the final 10,994 transcripts into 24 functional classes (Supplementary file 1). Notably, our classification strategy also includes the "unknown" class, which accounts for transcripts that were not classified within the other groups. Transcripts within this functional group are those that exhibited a high degree of similarity to previously deposited sequences of currently unknown function or displayed no or low similarities with previously deposited sequence, thereby representing

potential novel sequences from ticks. Remarkably, this functional class consistently emerged as the most abundant across all biological conditions, comprising 25 to 38 % of all transcripts (Fig. 2). This result underscores the overall knowledge gap in our understanding of tick physiology and emphasizes the necessity for further exploration of this tissue. Such exploration is significant not only in the context of the tick's life cycle but also in terms of pathogen acquisition, establishment, and transmission.

Furthermore, exploration of the relative abundance of each functional class across different feeding phases (Fig. 2) provides an overview of the dynamic changes that take place in the midgut, offering a glimpse of how important metabolic processes are temporally organized and transcribed in the tick midgut as feeding progresses. The "cytoskeletal" functional group, which contains transcripts coding for putative myosin, actin, tubulin, dynein, and other structural cellular components, was highly prevalent in the early stages of feeding, followed by a pronounced decrease at the 24-hpd group. A somewhat analogous trend was observed in the "extracellular matrix" functional group. This pattern appears to harmoniously align with the morphological changes that accompany the feeding progression of *R. microplus* adult females. It is reasonable to assume that during the slow-feeding phase, the tick must prepare to synthesize the necessary proteins to facilitate the expansion of its body. Furthermore, this "preparatory" phase assumes paramount importance, especially considering that tick engorgement occurs swiftly, necessitating the presence of all essential components for accommodating the blood meal.

In contrast, the "storage" functional class, which includes several lipoproteins, ferritins, and putative vitellogenins, displayed an inverted trend. It exhibited minimal expression during the initial feeding stages, followed by a consistent increase after tick detachment (Fig. 2s). This notable surge appears to represent the final steps of the blood meal digestion, as the tick initiates the synthesis of proteins capable of

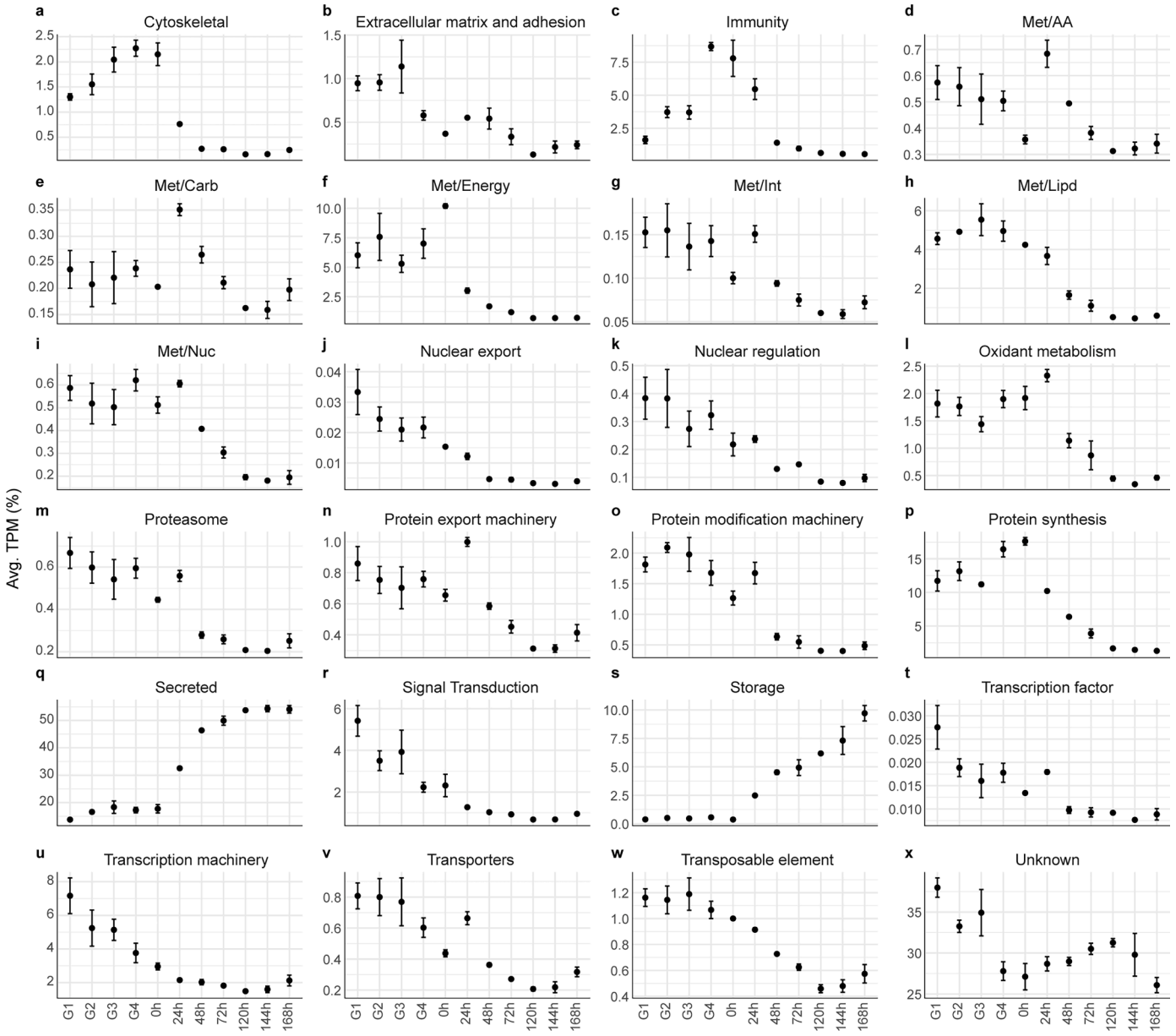

Fig. 2. Relative quantification of the 24 functional classes over the different biological groups of *Rhipicephalus microplus* midgut. Dots represent the average TPM (%) of each functional group. Errors bars represent the standard error of the mean. G1 – G4 indicate partially fed ticks that were collected and grouped based on their average weight; (G1) 38.9 ± 4.48 mg, (G2) 60.8 ± 10.1 mg, (G3) 94.7 ± 9.0 mg and (G4) 192.9 ± 12.4 mg. Meanwhile, 0 h – 168 h represent ticks collected at different time points after their natural detachment from their host.

binding and transporting heme, lipids, and carbohydrates, ultimately playing a pivotal role in heme acquisition (J. Perner et al., 2016) and embryo development (R.D. Mitchell et al., 2007). Notably, the majority of the functional classes exhibited a biphasic pattern, characterized by their abundance in the midgut of ticks prior to detachment, followed by a decrease after 24-hpd. Only the "secreted" and "storage" classes deviated from this trend, presenting an inverse profile (Fig. 2Q and 2S).

To systematically uncover the transcriptional changes induced by the blood meal at each phase of the tick feeding covered here, we performed pairwise differential expression analysis. This involved comparing the transcripts of each feeding stage with the preceding condition (Fig. 3). Analogous to our longitudinal analysis of *I. scapularis* midgut (Lu et al., 2023), we observed a limited number of differentially expressed transcripts throughout the slow-feeding stage, denoted here by the G1 to G3 groups, indicating an overall conserved transcriptional profile during the initial days of feeding. The comparison between G4 and G3 revealed the second-highest number of differentially expressed transcripts (247 in total, with 118 upregulated and 129 downregulated). Considering the average weight of ticks in the G3 (94.7 ± 9.0 mg) and G4 (192.9 ± 12.4 mg) groups, it is reasonable to suggest that this comparison partially characterizes the rapid feeding phase of *R. microplus* ticks. It is important to clarify the distinction between ticks in the G4 and 0 h groups. Currently, in our *R. microplus* feeding experiments on cattle, fully engorged female ticks exhibit a weight variation ranging from 187.5 to

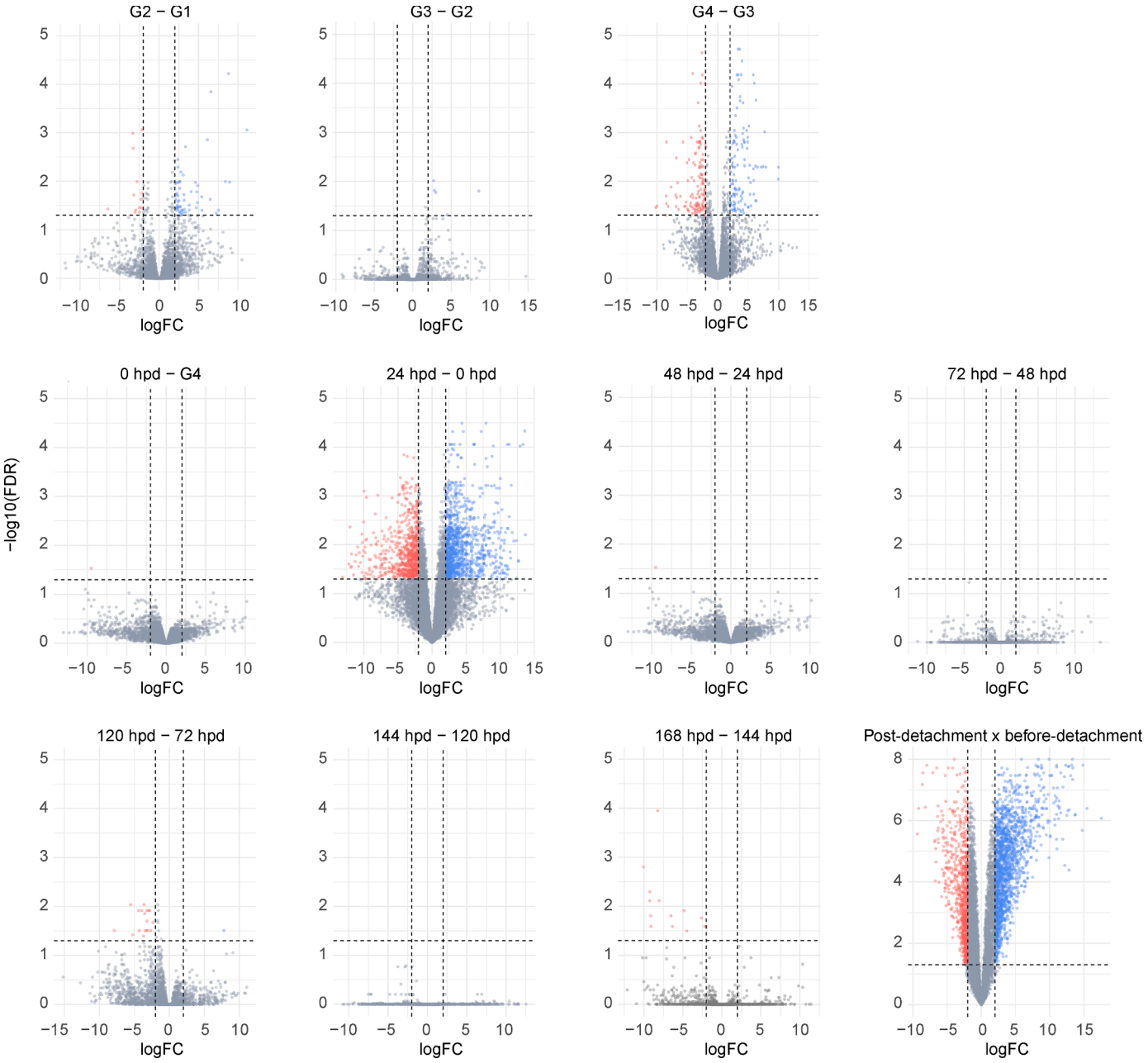

Fig. 3. Volcano plot panel illustrating the differentially expressed transcripts found between in *Rhipicephalus microplus* midgut collected at different feeding stages. Statistical difference was considered when a transcript presented a Log_2(Fold change) higher than 2 or lesser than –2 (vertical dotted lines) and a false discovery rate (FDR) ≤ 0.05 (horizontal dotted lines). Up-regulated transcripts are shown in blue, down-regulated transcripts are shown in red and transcripts that were not considered differentially expressed are shown as gray dots. G1 – G4 indicates partially fed ticks that were collected and grouped based on their average weight; (G1) 38.9 ± 4.48 mg, (G2) 60.8 ± 10.1 mg, (G3) 94.7 ± 9.0 mg and (G4) 192.9 ± 12.4 mg. Meanwhile, 0 h – 168 h represent ticks collected at different time points after their natural detachment from their host. The post detachment versus before detachment comparison includes 24–168 hpd versus G1–0-hpd groups.

312.5 mg, encompassing ticks in both G4 and 0 h. Therefore, the primary difference between these two groups lies in the fact that G4 ticks were still attached to the host during collection. However, it is plausible that such ticks are on the brink of detachment, which could explain the nearly identical transcriptional profile between the two groups (Fig. 1C and Fig. 3). This observation emphasizes the relationship between tick weight and the actual feeding stage, further reinforcing the concept that categorizing ticks based on their weight can provide accurate representations of their biological condition.

As expected, detachment of tick from their host, represented here by the 24-hpd versus 0-hpd comparison, is accompanied by the highest number of differentially expressed transcripts. In this context, there were 1696 upregulated and 775 downregulated transcripts observed. Subsequently, there are more subtle alterations observed up to the 48-hpd mark (Fig. 3). It is worth noting that the absence of differentially expressed transcripts in later time point comparisons can be attributed, in part, to the notable variability of our samples. This variance was particularly prominent within the 72-hpd and 144-hpd groups (Fig. 1B). Nonetheless, it is pertinent to consider that our multidimensional plot primarily segregates the fully engorged samples along dimension 2, which accounts for only 7 % of the overall variance (Fig. 1B). Based on dimensional analysis and our heatmap plot (Fig. 1C), it is plausible to suggest that the midgut transcriptional profiles of ticks during the later stages after detachment exhibit a certain degree of similarity.

Considering our initial data exploration (Fig. 1), which suggests the presence of two prominent transcriptional profiles, we chose to conduct a comparison between the midgut of ticks before detachment (G1 – 0 hour) and those post detachment (2 h – 168 h) (Fig. 3). This comparative analysis resulted in the identification of 2472 differentially expressed transcripts (Table 1). As expected, within this pool of modulated transcripts, a significant portion (580) was attributed to the "unknown" functional class. Subsequently, the second most prevalent modulated class was the "secreted" group, which contains transcripts commonly reported in the salivary glands of ticks (L. Tirloni et al., 2020; L. Tirloni et al., 2020; Ribeiro and Mans, 2020) encompassing peptidases, peptidases inhibitors, lipocalins, esterases, lipases, and mucins.

Table 1
Functional classification of the differentially expressed transcripts in the midgut of ticks from partially (PE) and fully (FE) engorged *Rhipicephalus microplus* ticks.

Class	No. of modulated transcripts		PE TPM[1]	FE TPM	FE/PE TPM
	Up	Down			
Cytoskeletal	48	17	2339.5	931.46	0.4
Extracellular matrix	33	11	4358.6	1815.4	0.42
Immunity	34	17	1340.8	4931.7	3.68
Met/aa	46	11	962.35	1735.6	1.8
Met/carb	43	9	285.27	1038	3.64
Met/energy	37	28	1159.2	395.38	0.34
Met/int	15	10	278.31	193.78	0.7
Met/lipd	80	23	2056.4	1725.4	0.84
Met/nuc	10	6	577.64	330.72	0.57
Nuclear export	0	7	39.95	3.51	0.09
Nuclear regulation	15	22	471.01	162.44	0.34
Oxidant metabolism	52	23	14,683	16,086	1.1
Proteasome	36	11	254.35	420.92	1.65
Protein export	103	13	820.78	1859.1	2.27
Protein modification	51	29	6222	2162.2	0.35
Protein synthesis	17	27	598.9	228.36	0.38
Secreted	290	151	79,560	444,002	5.58
Signal transduction	156	22	904.58	2781.2	3.07
Storage	10	4	1219.9	55,986	45.89
Transcription factor	2	1	6.27	6.33	1.01
Transcription machinery	87	55	2480.8	1485.7	0.6
Transporters	131	29	1894	1192	0.63
Transposable element	42	28	253.26	1170.2	4.62
Unknown	358	222	58,877	200,198	3.4

[1] TPM:Transcript per million.

Apart from establishing a foundational understanding of tick midgut physiology, the findings presented in this study hold implications for identifying potential targets that could be utilized in development of new approaches for tick control. The identification of new proteins plays a pivotal role in advancing tick vaccine and acaricide development, as these proteins hold the key to understanding tick biology, enabling targeted interventions that can mitigate the spread of tick-borne diseases and reduce the reliance on chemical control methods. Moreover, currently, the only commercially available anti-tick vaccine is based on the midgut protein Bm86 (Rand et al., 1989; Willadsen et al., 1989), which serves as a proof of concept for the use of midgut proteins in anti-tick control strategies. In the following subsections, we will focus on the three main transcriptional stages identified in *R. microplus* midgut, focusing on the differentially expressed transcripts and their potential role in tick physiology.

3.2. The partially fed stage

This phase accounts for a significant portion of the tick feeding cycle, spanning multiple days. During this stage, the tick gradually ingests moderate volumes of blood, leading to the steady expansion of the midgut lumen (Agyei and Runham, 1995). The host red blood cells are ruptured in the midgut lumen by a yet-to-be-discovered mechanism releasing hemoglobin, which is assimilated into larger endosomes within the digestive cells by an unknown, yet specific, cell receptor (Lara et al., 2005). During this stage, hemoglobin degradation becomes evident through the emergence of hemosomes, membrane-delimited organelles that contain vast amounts of heme (Lara et al., 2003).

Due to practical challenges associated with feeding *R. microplus* ticks on cattle, we were unable to collect unfed female adults. This observation bears relevance, as previous studies have demonstrated that the initial interaction between the tick midgut and the host's blood triggers substantial transcriptional changes within this organ (J. Perner et al., 2016; L. Tirloni et al., 2020; Stutzer et al., 2013). However, it was also recently demonstrated in *I. scapularis* midguts that a significant portion of such changes are maintained throughout the slow-feeding phase (Lu et al., 2023). Considering that only a marginal number of transcripts were found to be differentially expressed in the pairwise comparison of midgut from ticks within the slow-feeding phase (Fig. 3), it is likely that, similar to *I. scapularis*, the transcriptional changes induced by the blood meal of unfed *R. microplus* are sustained during the slow-feeding stage.

To systematically identify abundant transcripts in the different feeding stages, we conducted an unsupervised clustering of the final filtered putative CDS. This analysis resulted in the formation of five primary clusters (Fig. 4) based on the transcripts pattern across various biological conditions. Notably, cluster 1 contained 4703 transcripts and exhibited a predominant presence prior to tick detachment, with smaller abundance in the 0- and 24-hpd groups and negligible expression in subsequent time points. Cluster 2, comprising 1343 transcripts, exhibited marked abundance specifically within the 24-hpd group. Notably, transcripts grouped in clusters 3 (1428 transcripts), 4 (54 transcripts), and 5 (43 transcripts) exhibited high variability in their TPM values at all (cluster 3) or at specific time points (clusters 4 and 5, Fig. 4). Therefore, is likely that such clusters are artifacts of the unsupervised method utilized and do not provide substantial biological insights into *R. microplus* midgut physiology. As a result, similar to our previous analysis (PCA and differentially expression), the unsupervised clustering highlight two primary transcriptional patterns: one characterized by abundant transcripts prior to tick detachment (cluster 1), and another showcasing transcripts that are abundant in the early day post-detachment (cluster 2).

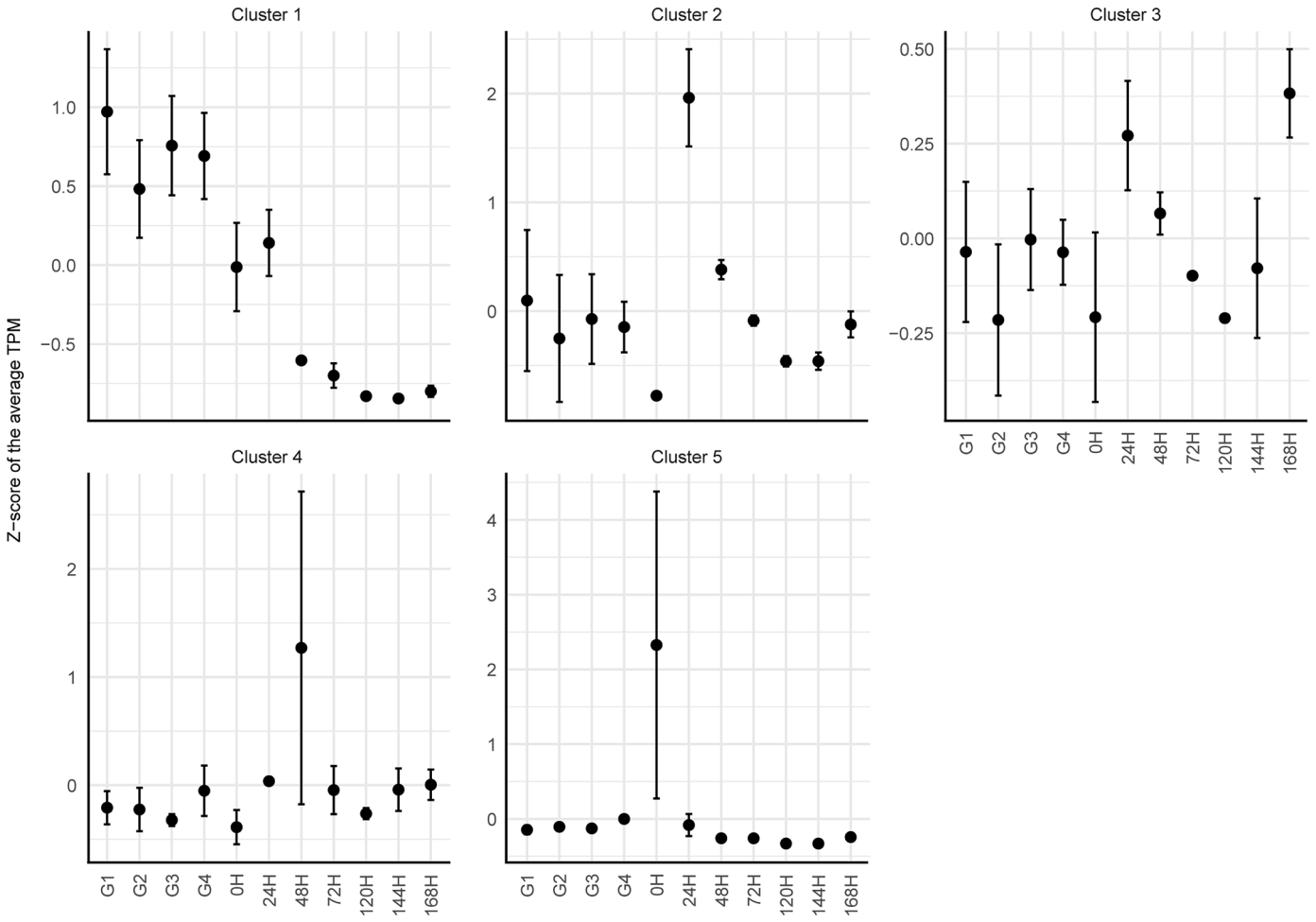

Fig. 4. Unsupervised clustering of the transcripts that presented an average transcript per million (TPM) ≥ 3 in the midgut of *Rhipicephalus microplus* midgut at different feeding conditions. The dots represent the average Z-score of the TPM from the transcripts contained within each cluster at each feeding stage. The errors bars represent the standard deviation of the mean.

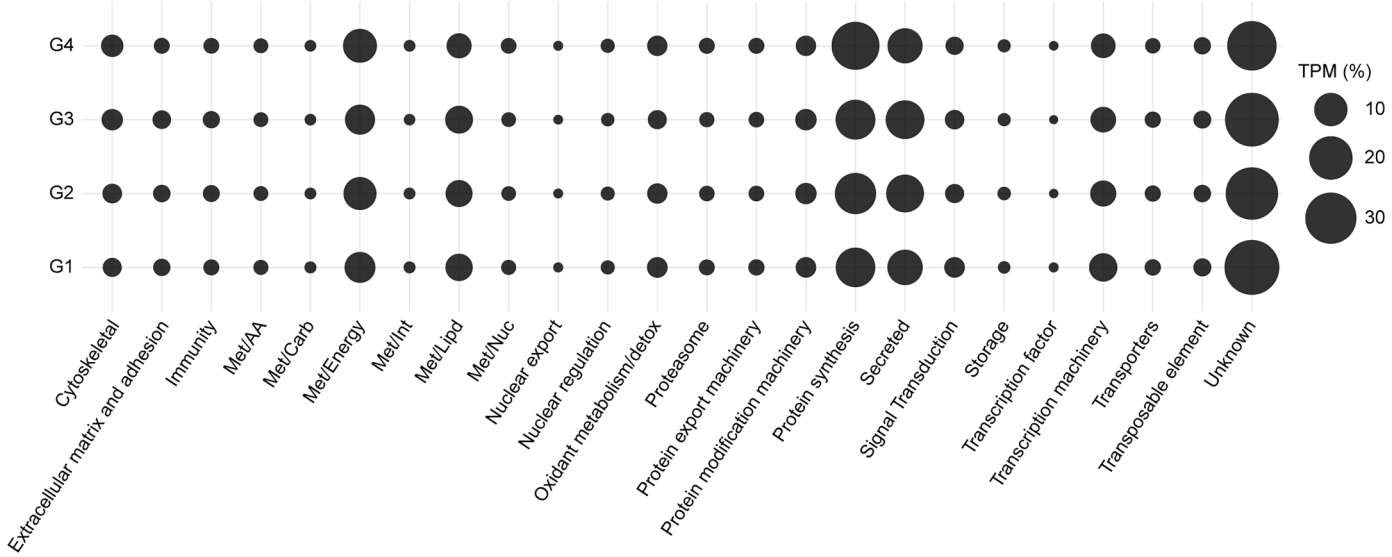

Fig. 5. Relative quantification of the 24 functional classes of *Rhipicephalus microplus* midgut transcripts within cluster 1. The average TPM, as percentage, is represented by the size of each sphere. G1 – G4 indicates partially fed ticks that were collected and grouped based on their average weight; (G1) 38.9 ± 4.48 mg, (G2) 60.8 ± 10.1 mg, (G3) 94.7 ± 9.0 mg and (G4) 192.9 ± 12.4 mg.

Consequently, to better describe the transcriptional profile of slow-feeding adult *R. microplus* females, we chose to focus on the transcripts present in the cluster 1, mainly those that were abundant in the G1 thought G4 groups. As expected, further exploration of the functional classification of these transcripts revealed a similar pattern in all four conditions, with the "unknown" (27 – 35 %), "protein synthesis" (15 – 25 %), "secreted" (11 – 14 %), and "energetic metabolism – Met/Energy" (7 – 10 %) classes being the most abundant (Fig. 5). The elevated presence of the "protein synthesis" class appears to reflect the active state of the tick midgut, where its machinery is constantly producing proteins necessary to accommodate and process the blood meal.

Within the "secreted" class, we have identified putative peptidases and peptidases inhibitors that play a pivotal role in the degradation of hemoglobin. In contrast to other hematophagous arthropods, ticks do not process their blood meal within the midgut lumen. Instead, intracellular hemoglobin digestion occurs in the digestive cells through cysteine and aspartic peptidases (Horn et al., 2009). As expected, we have uncovered several transcripts encoding putative cysteine (Supplementary figure 1) and aspartic peptidases (cathepsin D) with moderate to high levels of TPM throughout the slow-feeding phase (Supplementary figure 2). Furthermore, within the putative cathepsin D-like peptidases, Rm140393 and Rm140397 exhibited notable similarity to BmAP (*Boophilus microplus* Aspartic Peptidase), known to generate antimicrobial peptides (hemocidins) from hemoglobin (Cruz et al., 2010). Highlighting that such peptidases not only contribute to hemoglobin degradation but also to the tick's immune response. In the current dataset, BmAP (Rm140392) displayed substantial variability during the early feeding stages and is moderately abundant within the midgut of post-detached ticks. This observation aligns with the concept of "early" and "late" digestive peptidases, similar to what has been described in mosquitoes (Barillasmury et al., 1995) and kissing bugs (Henriques et al., 2020). This underscores the presence of a sophisticated regulatory mechanism that orchestrates blood meal digestion in ticks.

Within cluster 1, we have also detected multiple transcripts encoding putative serine peptidases from the MEROPS S01A subfamily, encompassing trypsins and chymotrypsin-like peptidases. It is worth noting that while most serine peptidases exhibited low TPM values, five presented moderate levels, of which four were found in cluster 1 (Rm114855, Rm135900, Rm32624 and seqSigP-43,736) (Supplementary figure 3). Although similar transcripts have been reported in previous RNA-sequencing studies of tick midgut (J. Perner et al., 2016; Lu et al., 2023; L. Tirloni et al., 2020), their contribution to blood meal digestion remains unclear. Recent finds have indicated that midgut extracts from unfed and partially fed *I. scapularis* adults lack trypsin-like activity, but this activity is present in detached ticks (Reyes et al., 2020). Although, an in-depth biochemical characterization of *R. microplus* peptidase activity at different feeding stages is not available, based on the moderate levels of TPM, it is possible that these transcripts might not undergo translation or that the proteins are maintained as zymogens during the early feeding stages.

Lastly, in addition to the peptidases, we also observed multiple serine and cysteine peptidases inhibitors. Within the serine peptidase inhibitors, cluster 1 presented moderate levels of transcripts encoding putative serpins and Kunitz-type inhibitors (Supplementary file 1). These inhibitors are thought to serve as regulators of host serine peptidases involved in hemostasis (e.g., thrombin), thereby promoting the maintenance of the ingested blood in a fluid state (Soares et al., 2012; Liao et al., 2009). Corroborating with this notion, all transcripts encoding putative Kunitz-type inhibitors within cluster 1 possess an Arg-residue at their P1 position, strongly suggesting that they could act as thrombin inhibitors. This mechanism, in turn, would favor the digestion and processing of the blood meal. Furthermore, among the inhibitors, we have observed the presence of cystatins, which are tight-binding cysteine peptidase inhibitors. The cystatins are traditionally categorized into three subfamilies based on their molecular weight and number of disulfide bridges (Barrett et al., 1986). Currently, multiple type-1 and type-2 cystatins from *R. microplus* midgut have been characterized (Lima et al., 2006; Parizi et al., 2013) and suggested to function as endogenous regulators of tick cysteine peptidases (Parizi et al., 2015; Cardoso et al., 2017), in addition to potentially interfering with peptidases originating from tick-borne pathogens (Lu et al., 2020; Wei et al., 2020).Beyond providing a basic understanding of tick midgut physiology, the current dataset can also be leveraged for the identification of antigens suitable for the development of anti-tick control methods. Disrupting the activity of proteins within cluster 1 could potentially impede the initial feeding stages of ticks, thereby preventing significant harm to the cattle. As of now, the sole commercially available vaccine is based on the midgut protein Bm86 (Willadsen et al., 1989). Furthermore, Bm86 (Rm132620, Supplementary figure 4) was clustered within cluster 1, indicating that it is more abundant in the early feeding stages of *R. microplus*. (Pipano et al., 2003) This observation underscores a proof of concept, suggesting that targeting midgut proteins abundant in the slow-feeding phase could prove to be a potent strategy for tick control.

3.3. Rapid-feeding stage

During this phase, the mated female tick ingests a substantial volume of blood within a relatively brief period, spanning from 12 to 24 h (Roberts, 1968). This phase of rapid feeding is accompanied by a drastic expansion of the tick's body size, resulting in an increase of nearly 100 times in its overall body weight (Sonenshine, 2013).

Functional classification of the 248 differentially expressed transcripts between the G4 and G3 ticks revealed a prevailing down-regulation trend ($G4_{TPM}/G3_{TPM} < 1$, table 2). This observation suggests that, as ticks approach the fully engorged state, a shift occurs in the overall transcriptional activity within the midgut. Notably, a similar trend was also observed in the midgut of *I. scapularis* adult females (Lu et al., 2023), indicating the conservation of this transcriptional regulation pattern across ticks of different species. Upon closer inspection of the TPM ratios between the G4 and G3 groups, we observed that the most upregulated functional classes were "energetic metabolism – Met/Energy", "storage" and "oxidant metabolism" (Table 2). However, it is important to note that, with exception of the "oxidant metabolism"

Table 2
Functional classification of the differentially expressed transcripts in the midgut of *Rhipicephalus microplus* ticks from G4 and G3 groups.

Class	No. of modulated transcripts		G3 TPM[1]	G4 TPM	G4/G3
	Up	Down			
Met/energy	1	0	0.01	0.36	53.50
Storage	1	0	35.75	663.85	18.57
Oxidant metabolism	4	2	123.4	1829.2	14.83
Met/int	3	0	5.54	75.71	13.66
Transcription machinery	1	0	0.39	3.82	9.72
Transposable element	4	1	25.06	124.29	4.96
Met/carb	4	0	18.39	91.02	4.95
Met/aa	2	1	23.18	104.70	4.52
Transporters	12	11	130.02	361.87	2.78
Unknown	33	35	38,190.6	27,915.78	0.73
Signal transduction	4	2	44.59	19.05	0.43
Immunity	9	9	2048.16	832.27	0.41
Met/lipd	4	7	268.21	98.26	0.37
Secreted	33	51	53,404.6	16,584.51	0.31
Extracellular matrix	3	6	7506.68	1378.17	0.18
Protein modification machinery	1	1	90.43	12.40	0.14
Protein export machinery	0	1	4.88	0.56	0.11
Cytoskeletal	0	1	1.11	0.00	0.00
Nuclear regulation	0	1	1.96	0.00	0.00

[1] TPM:Transcript per million.

class, these classes displayed overall low TPM levels, which may not accurately reflect the major transcriptional changes occurring in the tick midgut during the rapid-feeding phase. When considering moderate levels of TPM, it becomes evident that the most affected classes are "unknown", "secreted", and "oxidant metabolism" (Table 2).

As feeding progresses, the degradation of hemoglobin is followed by the release of significant amounts of heme that can potentially induce oxidative damage (Citelli et al., 2007). During the rapid-feeding phase, we observed two transcripts coding for putative glutathione S-transferases (GSTs) that were highly modulated (LogFC ~ 4.1). GSTs are found in all eukaryotes and are responsible for elimination of toxic substances (Shahein et al., 2008). In ticks, they have been implicated with permethrin detoxification, pyrethroid resistance, and antioxidant responses (Duscher et al., 2014; Nandi et al., 2015; Freitas et al., 2007) Therefore, it appears that their increased transcription during this feeding stages is likely a response to the increase of heme-related oxidative stress originated from hemoglobin digestion.

As mentioned previously, the "secreted" class contains proteins bearing a putative signal peptide. Although we observed an overall reduction of this functional group during the rapid-feeding phase (Table 2), we also observed multiple transcripts encoding putative peptidases and peptidases inhibitors that were upregulated. Notably, three putative cathepsin D-like peptidases (Rm102236, Rm51154 and Rm57951) exhibited moderate to high values of TPM in ticks belonging to the G4 group. Furthermore, these three transcripts were not identified among those observed during the slow-feeding phase (Supplementary figure 2). Upon comparing the transcriptional pattern of these enzymes, it becomes evident that they are divided into two groups, "early" and "late", with Rm102236, Rm51154 and Rm57951 belonging to the latter. A similar dichotomic pattern was also found for multiple transcripts encoding putative serine peptidase inhibitors from the Kunitz-type subfamily (Supplementary figure 5), in which the ones prevalent during the slow-feeding phase were distinct from those in the rapid-feeding stage. Moreover, peptidase inhibitors can be important in tick vaccine development (de la Fuente et al., 2008; Parizi et al., 2020; Costa et al., 2023) as they enable the precise modulation of key biological processes, offering a promising strategy for disrupting tick-borne pathogens transmission and enhancing vaccine efficacy.

Lastly, the presence of "early" and "late" inhibitors underscores the notion that a specific regulatory mechanism governing not only peptidases but also peptidase inhibitors are present in the tick midgut. Further studies focused on the identification and characterization of promoters and transcription factors are likely to be the next steps in our quest to comprehend the triggers and signals that temporally regulate the expression of peptidases and peptidase inhibitors orchestrating blood meal digestion in ticks.

The collection of ticks that distinctly characterizes the demarcation between the slow- and rapid-feeding phases is challenging due to their close temporal proximity. This is particularly true in the case of *R. microplus*, which is a one-host tick that feeds exclusively on cattle, introducing additional practical difficulties. As a consequence, the current dataset provides only a partial representation of the rapid feeding phase through the comparison between the G4 and G3 groups, which accounted for the second highest number of differentially expressed transcripts (Fig. 3 and Table 2). Consequently, further studies focusing on the collection of ticks weighting between 100 and 190 mg are necessary to provide a higher resolution regarding the intricate alterations that unfold in the tick midgut during the transition from the slow- to the rapid-feeding stages.

3.4. The detachment and post-detachment stages

Tick detachment stands as a significant milestone in the tick life cycle, occurring after completion of feeding. Within the present dataset, this phase is represented through the 24-hpd and 0-hpd comparison, which yields the highest number of differentially expressed transcripts (Fig. 3). Among the 1760 modulated transcripts between the 24-hpd/0-hpd groups, we observed that the most upregulated transcripts with moderate to high TPM values belonged to the "storage", "immunity", and "secreted" functional classes (Table 3).

Table 3
Functional classification of the differentially expressed transcripts in the midgut of *Rhipicephalus microplus* ticks from 24-hpd and 0-hpd groups.

Class	No. of modulated transcripts		0-hpd TPM[1]	24-hpd TPM	24-hpd/0-hpd
	Up	Down			
Storage	5	0	529.48	18,844.78	35.59
Transcription factor	1	0	1.235	11.345	9.19
Immunity	17	5	208.05	1499.185	7.21
Secreted	167	131	27,372.11	165,198.9	6.04
Protein export machinery	63	5	466.82	2320.03	4.97
Met/carb	29	2	168.25	777.13	4.62
Met/lipd	51	8	353.025	1477.67	4.19
Extracellular matrix	34	7	298.655	1179.875	3.95
Met/aa	29	5	499.67	1664.375	3.33
Met/nuc	12	7	222.66	737.32	3.31
Met/int	11	3	59.495	188.29	3.16
Transporters	69	13	553.71	1008.33	1.82
Proteasome	24	17	655.015	757.895	1.16
Protein modification	28	11	1747.45	1518.75	0.87
Unknown	234	307	118,770.7	101,993.5	0.86
Nuclear regulation	16	10	201.025	150.195	0.75
Transposable element	31	37	974.95	584.995	0.60
Nuclear export	1	2	22.505	10.485	0.47
Transcription machinery	58	28	5402.18	1946.09	0.36
Oxidant metabolism	27	8	82,256.12	27,612.92	0.34
Signal transduction	79	14	16,454.48	5026.965	0.31
Protein synthesis	18	35	33,321.93	9689.125	0.29
Cytoskeletal	39	17	17,401.63	3283.835	0.19
Met/energy	23	22	79,090.43	14,026.96	0.18

[1] TPM:Transcript per million.

Within the "storage" class, we identified five upregulated transcripts. However, two of them, Rm22740 and Rm98262, account for 99.6 % of the total TPM for this class, and both encode putative hemelipoproteins (Supplementary file 1). These proteins typically exhibit a high molecular weight (>200 kDa) and are associated with heme, lipid, and carbohydrate binding. In ticks, it has been demonstrated that hemelipoproteins are primarily synthesized in the fat body while the midgut is considered a secondary production organ (Khalil et al., 2011; R.D. Mitchell et al., 2007). While traditionally associated with embryo development (Umemiya-Shirafuji et al., 2019; Seixas et al., 2018), the notable abundance of these hemelipoproteins in the midgut at this feeding stage suggests a different role – specifically, their involvement in heme binding. At this point in the tick's feeding cycle, the midgut displays its highest proteolytic activity (Franta et al., 2010), indicating rapid degradation of hemoglobin, which is followed by the release vast amounts of heme. Consequently, it is likely that Rm22740 and Rm98262 serve as detoxification proteins by binding to heme. Furthermore, it is likely that they are also related to the acquisition and distribution of heme. This function is particularly critical for the tick physiology since ticks lack the capability to produce heme on their own (J. Perner et al., 2016; Braz et al., 1999).

During the initial 24-hpd, the second most modulated functional class was the "immunity" group, showing a 7.2-fold increase (Table 3). Within this category we observed multiple transcripts that encode putative microplusin-like antimicrobial peptides (Supplementary file 1). Microplusin was originally isolated from the hemolymph of *R. microplus* and demonstrated to possess antimicrobial activity against gram-positive bacteria (Fogaca et al., 2004). Further investigations have suggested that microplusin's bacteriostatic activity can be attributed to the presence of histidine-rich regions within the peptide. These regions

have the capability to bind and sequester metal ions, such as copper (Silva et al., 2009). The heightened transcription of antimicrobial peptides at this stage is likely linked to the accumulating blood meal in the tick midgut lumen, creating a favored environment for the proliferation of bacteria and/or other microorganism that requires regulation.

Finally, within the upregulated transcripts of the "secreted" class, similar to previous feeding stages, we have identified multiple serine peptidase inhibitors from the Kunitz-type subfamily, along with several digestive peptidases, including putative legumains, cathepsins D and L. This high abundance of digestive peptidases suggests that the midgut of fully engorged *R. microplus* adults exhibits its highest proteolytic activity, similar to what has been shown to *Ixodes ricinus* (Franta et al., 2010). Notably, *R. microplus* possesses a substantial number of transcripts coding for putative Kunitz-type inhibitors. Most of the inhibitors that were upregulated in the rapid feeding phase displayed even higher TPM values in fully fed ticks (Supplementary file 1). Furthermore, upon inspecting their putative P1 residues, it becomes evident that these inhibitors likely target multiple serine peptidases. This is supported by the identification of P1 residues such as val, ser, gly, arg, lys, met, asn and tyr (Supplementary file 1). Therefore, it is possible that these Kunitz inhibitors possess the capability to inhibit other host serine peptidase cascades that could potentially pose a threat to the tick midgut, such as complement activation and neutrophil degranulation (Barros et al., 2009). Further investigations focused on these inhibitors will enhance our comprehension of their broader role in tick midgut physiology.

Notably, when extending our analysis to the midgut of ticks up to 168-hpd, we observed a moderate number of modulated transcripts only up to 48-hpd (Table 4), with little to no difference at later time points (Fig. 3). This overall absence of differentially expressed transcripts in post-detached ticks suggests that the midgut maintains a conserved transcriptional profile beyond 48-hpd.

The 48-hpd/24-hpd comparison exhibits an overall reduction in the transcriptional activity within the tick midgut. Most of the functional classes show a downregulation trend (Table 4). The exceptions to this pattern included the "lipid metabolism – Met/Lipd", "amino acid metabolism – Met/AA", and "secreted" classes. However, it is worth noting that only the "secreted" class exhibits moderately high levels of TPM at approximately 3000. Among the most abundant transcripts in this class are Rm145420 and Rm20292, which encode putative type-1 cystatins. As previously mentioned, these intracellular cysteine peptidase inhibitors are recognized as regulators of tick digestive peptidases (Parizi et al., 2015; Lu et al., 2020). Therefore, their upregulation likely signifies the onset of the final stages of hemoglobin digestion, during which peptidase activity must be carefully controlled to prevent unintended proteolysis. This event aligns with the macroscopic changes observed in the tick midgut, which gradually decreases in size and mass at later time points post-detachment.

4. Conclusion

Tick feeding is divided into three key stages: a preparatory stage during which the tick attaches to its host and creates the feeding lesion, a slow-feeding stage spanning multiples days, and a rapid-feeding stage in which the adult female ingests a large volume of blood in a short-time frame. Here, a comprehensive longitudinal transcriptome analysis of the midgut from adult female *R. microplus* ticks collected at various feeding stages was performed. We have identified distinct transcriptional profiles that can be associated with both the slow- and rapid-feeding stages. Furthermore, our observations reveal that the initial days following tick detachment (up to 48 h) exhibit the highest number of differentially expressed transcripts. However, no major transcriptional changes were noted in subsequent periods. This temporal, organ-specific dataset serves as a robust reference for investigating crucial aspects of tick midgut physiology in addition to favor the identification of potential targets that could be used to inform anti-tick control methods.

Table 4
Functional classification of the differentially expressed transcripts in the midgut of *Rhipicephalus microplus* ticks from 48-hpd and 24-hpd groups.

Class	No. of modulated transcripts		24-hpd TPM[1]	48-hpd TPM	48-hpd/24-hpd
	Up	Down			
Met/lipd	2	1	43.715	210.6267	4.82
Met/aa	2	1	59.24	209.49	3.54
Secreted	13	7	1332.13	3050.42	2.29
Unknown	14	34	3272.56	3092.223	0.94
Protein modification	1	7	471.13	124.0133	0.26
Immunity	2	3	17,126.88	2589.507	0.15
Cytoskeletal	0	4	1087.23	137.76	0.13
Oxidant metabolism	2	6	2316.165	270.29	0.12
Signal transduction	0	4	12.93	1.366667	0.11
Storage	0	1	381.1	40.10333	0.11
Nuclear export	0	3	9.395	0.973333	0.10
Transcription machinery	0	18	570.12	57.03667	0.10
Met/int	0	2	32.775	2.91	0.09
Nuclear regulation	0	3	18.91	1.666667	0.09
Protein export	0	2	8.04	0.536667	0.07
Proteasome	0	1	1.07	0.063333	0.06
Protein synthesis	0	4	10.58	0.6	0.06
Met/nuc	0	2	43.495	2.156667	0.05
Met/carb	0	1	1.61	0.076667	0.05
Transporters	1	3	111.65	3.246667	0.03
Met/energy	0	3	71.3	0.963333	0.01
Transposable element	0	1	1.625	0	0.00

[1] TPM:Transcript per million.

Author agreement statement

We the undersigned declare that this manuscript is original, has not been published before and is not currently being considered for publication elsewhere. We confirm that the manuscript has been read and approved by all named authors and that there are no other persons who satisfied the criteria for authorship but are not listed. We further confirm that the order of authors listed in the manuscript has been approved by all of us. We understand that the Corresponding Author is the sole contact for the Editorial process. He is responsible for communicating with the other authors about progress, submissions of revisions and final approval of proofs. Signed by all authors as follows:

Authors' contribution

Conceived and designed the experiments: SL, JW, LFP, ISV and LT Performed the experiments: SL, JW and LFP Contributed reagents/materials/analysis tools: SL, JW, LFP, ISV and LT Drafting the article: SL, JW, LFP, and ISV Critical revision of the article: SL, JW, LFP, ISV and LT

Data availability

The transcriptome data have been deposited in the National Center for Biotechnology Information (NCBI) under BioProject PRJNA1013468, with Biosamples SAMN37298818 - SAMN37298849. The raw reads have been submitted to the Sequence Reads Archives (SRA) under accessions SRR25925960 - SRR25925991.

Acknowledgments

We would like to acknowledge Dr. Jose M.C. Ribeiro for his support in this project and Alexander Stewart, Austin Athman, and Anita Mora from the Visual and Medical Arts branch (RTB, NIAID, NIH) for figure preparation. This work utilized the computational resources of the NIH HPC Biowulf cluster (http://hpc.nih.gov). LT was supported by the Intramural Research Program of the National Institute of Allergy and

Infectious Diseases (grant Z01 AI001337-01). This work was supported by grants from Conselho Nacional de Desenvolvimento Científico e Tecnológico (CNPq) 405763/2018-2, 302360/2018-2, INCT-EM (Instituto Nacional de Ciência e Tecnologia de Entomologia Molecular) 465678/2014-9, Coordenação de Aperfeiçoamento de Pessoal de Nível Superior (CAPES) 88881.153222/2017-01, and Fundação de Amparo à Pesquisa do Estado do Rio Grande do Sul (FAPERGS) 21/2551-0002221-3 (Brazil).

Supplementary materials

Supplementary material associated with this article can be found, in the online version, at doi:10.1016/j.ttbdis.2023.102304.

References

Agyei, A.D., Runham, N.W., 1995. Studies on the morphological changes in the midguts of two ixodid tick species *Boophilus microplus* and *Rhipicephalus appendiculatus* during digestion of the blood meal. Int. J. Parasitol. 25, 55–62.

Agyei, A.D., Herbert, I.V., Runham, N.W., 1991. Histochemical localisation of acid phosphatase and non-specific esterase in the midguts of two species of tick, *Boophilus microplus* and *Rhipicephalus appendiculatus*, as determined by light microscopy. Parasitol. Res. 77, 629–634.

Andreotti, R., 2006. Performance of two Bm86 antigen vaccin formulation against tick using crossbreed bovines in stall test. Rev. Bras. Parasitol. Vet. 15, 97–100.

Barillasmury, C.V., Noriega, F.G., Wells, M.A., 1995. Early trypsin activity is part of the signal-transduction system that activates transcription of the late trypsin gene in the midgut of the mosquito. *Aedes-Aegypti. Insect. Biochem. Mol.* 25, 241–246.

Barrett, A.J., Fritz, H., Grubb, A., Isemura, S., Jarvinen, M., Katunuma, N., Machleidt, W., Muller-Esterl, W., Sasaki, M., Turk, V., 1986. Nomenclature and classification of the proteins homologous with the cysteine-proteinase inhibitor chicken cystatin. Biochem. J. 236, 312.

Barros, V.C., Assumpcao, J.G., Cadete, A.M., Santos, V.C., Cavalcante, R.R., Araujo, R.N., Pereira, M.H., Gontijo, N.F., 2009. The Role of Salivary and Intestinal Complement System Inhibitors in the Midgut Protection of Triatomines and Mosquitoes. PLoS ONE 4.

Becker, S., Webster, A., Doyle, R.L., Martins, J.R., Reck, J., Klafke, G.M., 2019. Resistance to deltamethrin, fipronil and ivermectin in the brown dog tick, *Rhipicephalus sanguineus* sensu stricto, Latreille (Acari: ixodidae). Ticks Tick Borne Dis. 10, 1046–1050.

Bendtsen, J.D., Nielsen, H., von Heijne, G., Brunak, S., 2004. Improved prediction of signal peptides: SignalP 3.0. J. Mol. Biol. 340, 783–795.

Braz, G.R.C., Coelho, H.S.L., Masuda, H., Oliveira, P.L., 1999. A missing metabolic pathway in the cattle tick *Boophilus microplus*. Curr. Biol. 9, 703–706.

Cardoso, T.H.S., Lu, S., Gonzalez, B.R.G., Torquato, R.J.S., Tanaka, A.S., 2017. Characterization of a novel cystatin type 2 from *Rhipicephalus microplus* midgut. Biochimie 140, 117–121.

Citelli, M., Lara, F.A., Vaz, I.D., Oliveira, P.L., 2007. Oxidative stress impairs heme detoxification in the midgut of the cattle tick, *Rhipicephalus (Boophilus) microplus*. Mol. Biochem. Parasit. 151, 81–88.

Costa, G.C.A., Silva, F.A.A., Manzato, V.M., Torquato, R.J.S., Gonzalez, Y.G., Parizi, L.F., Vaz, I.D., Tanaka, A.S., 2023. A multiepitope chimeric antigen from *Rhipicephalus microplus*-secreted salivary proteins elicits anti-tick protective antibodies in rabbit. Vet. Parasitol. 318.

Cruz, C.E., Fogaca, A.C., Nakayasu, E.S., Angeli, C.B., Belmonte, R., Almeida, I.C., Miranda, A., Miranda, M.T., Tanaka, A.S., Braz, G.R., Craik, C.S., Schneider, E., Caffrey, C.R., Daffre, S., 2010. Characterization of proteinases from the midgut of *Rhipicephalus (Boophilus) microplus* involved in the generation of antimicrobial peptides. Parasit. Vectors 3, 63.

de la Fuente, J., Maritz-Olivier, C., Naranjo, V., Ayoubi, P., Nijhof, A.M., Almazan, C., Canales, M., de la Lastra, J.M.P., Galindo, R.C., Blouin, E.F., Gortazar, C., Jongejan, F., Kocan, K.M., 2008. Evidence of the role of tick subolesin in gene expression. BMC Genomics 9.

Duscher, G.G., Galindo, R.C., Tichy, A., Hummel, K., Kocan, K.M., de la Fuente, J., 2014. Glutathione S-transferase affects permethrin detoxification in the brown dog tick, *Rhipicephalus sanguineus*. Ticks Tick-Borne Dis. 5, 225–233.

Fogaca, A.C., Lorenzini, D.M., Kaku, L.M., Esteves, E., Bulet, P., Daffre, S., 2004. Cysteine-rich antimicrobial peptides of the cattle tick *Boophilus microplus*: isolation, structural characterization and tissue expression profile. Dev. Comp. Immunol. 28, 191–200.

Franta, Z., Frantova, H., Konvickova, J., Horn, M., Sojka, D., Mares, M., and Kopacek, P. (2010) Dynamics of digestive proteolytic system during blood feeding of the hard tick Ixodes ricinus. Parasite vector 3.

Freitas, D.R.J., Rosa, R.M., Moraes, J., Campos, E., Logullo, C., Vaz, I.D., Masuda, A., 2007. Relationship between glutathione S-transferase, catalase, oxygen consumption, lipid peroxidation and oxidative stress in eggs and larvae of *Boophilus microplus* (Acarina: ixodidae). Comp. Biochem. Phys. A 146, 688–694.

Fu, L., Niu, B., Zhu, Z., Wu, S., Li, W., 2012. CD-HIT: accelerated for clustering the next-generation sequencing data. Bioinformatics 28, 3150–3152.

Grabherr, M.G., Haas, B.J., Yassour, M., Levin, J.Z., Thompson, D.A., Amit, I., Adiconis, X., Fan, L., Raychowdhury, R., Zeng, Q.D., Chen, Z.H., Mauceli, E., Hacohen, N., Gnirke, A., Rhind, N., di Palma, F., Birren, B.W., Nusbaum, C., Lindblad-Toh, K., Friedman, N., Regev, A., 2011. Full-length transcriptome assembly from RNA-Seq data without a reference genome. Nat. Biotechnol. 29, 644–U130.

Grisi, L., Leite, R.C., Martins, J.R.D., de Barros, A.T.M., Andreotti, R., Cancado, P.H.D., de Leon, A.A.P., Pereira, J.B., Villela, H.S., 2014. Reassessment of the potential economic impact of cattle parasites in Brazil. Rev. Bras. Parasitol. V 23, 150–156.

Henriques, B.S., Gomes, B., Oliveira, P.L., Garcia, E.S., Azambuja, P., Genta, F.A., 2020. Characterization of the temporal pattern of blood protein digestion in *rhodnius prolixus*: first description of early and late gut cathepsins. Front. Physiol. 11, 509310.

Horn, M., Nussbaumerova, M., Sanda, M., Kovarova, Z., Srba, J., Franta, Z., Sojka, D., Bogyo, M., Caffrey, C.R., Kopacek, P., Mares, M., 2009. Hemoglobin digestion in blood-feeding ticks: mapping a multipeptidase pathway by functional proteomics. Chem. Biol. 16, 1053–1063.

Karim, S., Singh, P., Ribeiro, J.M.C., 2011. A Deep Insight into the Sialotranscriptome of the Gulf Coast Tick, *Amblyomma maculatum*. PLoS ONE 6.

Khalil, S.M.S., Donohue, K.V., Thompson, D.M., Jeffers, L.A., Ananthapadmanaban, U., Sonenshine, D.E., Mitchell, R.D., Roe, R.M., 2011. Full-length sequence, regulation and developmental studies of a second vitellogenin gene from the American dog tick, *Dermacentor variabilis*. J. Insect Physiol. 57, 400–408.

Landulfo, G.A., Patane, J.S.L., Silva, D., Junqueira-de-Azevedo, I.L.M., Mendonca, R.Z., Simons, S.M., Carvalho, E., Barros-Battesti, D.M., 2017. Gut transcriptome analysis on females of *Ornithodoros mimon* (Acari: argasidae) and phylogenetic inference of ticks. Rev. Bras. Parasitol. Vet. 26, 185–204.

Lara, F.A., Lins, U., Paiva-Silva, G., Almeida, I.C., Braga, C.M., Miguens, F.C., Oliveira, P. L., Dansa-Petretski, M., 2003. A new intracellular pathway of haem detoxification in the midgut of the cattle tick *Boophilus microplus*: aggregation inside a specialized organelle, the hemosome. J. Exp. Biol. 206, 1707–1715.

Lara, F.A., Lins, U., Bechara, G.H., Oliveira, P.L., 2005. Tracing heme in a living cell: hemoglobin degradation and heme traffic in digest cells of the cattle tick *Boophilus microplus*. J. Exp. Biol. 208, 3093–3101.

Lew-Tabor, A.E., Valle, M.R., 2016. A review of reverse vaccinology approaches for the development of vaccines against ticks and tick borne diseases. vol 7, pg 573, 2016 Ticks Tick-Borne Dis. 7, 1236–1237.

Li, B., Dewey, C.N., 2011. RSEM: accurate transcript quantification from RNA-Seq data with or without a reference genome. BMC Bioinformat. 12.

Li, A.Y., Chen, A.C., Miller, R.J., Davey, R.B., George, J.E, 2007. Acaricide resistance and synergism between permethrin and amitraz against susceptible and resistant strains of *Boophilus microplus* (Acari: ixodidae). Pest. Manag. Sci. 63, 882–889.

Liao, M., Zhou, J., Gong, H., Boldbaatar, D., Shirafuji, R., Battur, B., Nishikawa, Y., Fujisaki, K., 2009. Hemalin, a thrombin inhibitor isolated from a midgut cDNA library from the hard tick *Haemaphysalis longicornis*. J. Insect Physiol. 55, 164–173.

Lima, C.A., Sasaki, S.D., Tanaka, A.S., 2006. Bmcystatin, a cysteine proteinase inhibitor characterized from the tick *Boophilus microplus*. Biochem. Biophys. Res. Commun. 347, 44–50.

Lu, S., Rocha, da, L, A., Torquato, R.J.S., da Silva Vaz Junior, I., Florin-Christensen, M., Tanaka, A.S, 2020. A novel type 1 cystatin involved in the regulation of *Rhipicephalus microplus* midgut cysteine proteases. Ticks Tick Borne Dis. 11, 101374.

Lu, S., Martins, L.A., Kotal, J., Ribeiro, J.M.C., Tirloni, L., 2023. A longitudinal transcriptomic analysis from unfed to post-engorgement midguts of adult female *Ixodes scapularis*. Sci. Rep. 13, 11360.

Maeda, H., Hatta, T., Alim, M.A., Tsubokawa, D., Mikami, F., Kusakisako, K., Matsubayashi, M., Umemiya-Shirafuji, R., Tsuji, N., Tanaka, T., 2017. Initial development of *Babesia ovata* in the tick midgut. Vet. Parasitol. 233, 39–42.

Mans, B.J., Francischetti, I.M.B., 2016. Sialomic perspectives on the evolution of blood-feeding behavior in arthropods: future therapeutics by natural design. Toxins and Hemostasis. Springer, Dordrecht (R. Manjunatha Kini, K. J. C., Francis S. Markland, Mary Ann McLane, Takashi Morita ed.)pp.

Mans, B.J., 2011. Evolution of vertebrate hemostatic and inflammatory control mechanisms in blood-feeding arthropods. J. Innate Immun. 3, 41–51.

3rd Mitchell, R.D., Ross, E., Osgood, C., Sonenshine, D.E., Donohue, K.V., Khalil, S.M., Thompson, D.M., Michael Roe, R, 2007a. Molecular characterization, tissue-specific expression and RNAi knockdown of the first vitellogenin receptor from a tick. Insect Biochem. Mol. Biol. 37, 375–388.

Mitchell, R.D., Ross, E., Osgood, C., Sonenshine, D.E., Donohue, K.V., Khalil, S.M., Thompson, D.M., Roe, R.M., 2007b. Molecular characterization, tissue-specific expression and RNAi knockdown of the first vitellogenin receptor from a tick. Insect. Biochem. Mol. 37, 375–388.

Nandi, A., Jyoti, Singh, H., Singh, N.K, 2015. Esterase and glutathione S-transferase levels associated with synthetic pyrethroid resistance in *Hyalomma anatolicum* and *Rhipicephalus microplus* ticks from Punjab, India. Exp. Appl. Acarol. 66, 141–157.

Pal, U., Li, X., Wang, T., Montgomery, R.R., Ramamoorthi, N., Desilva, A.M., Bao, F., Yang, X., Pypaert, M., Pradhan, D., Kantor, F.S., Telford, S., Anderson, J.F., Fikrig, E., 2004. TROSPA, an *Ixodes scapularis* receptor for *Borrelia burgdorferi*. CellCell 119, 457–468.

Parizi, L.F., Githaka, N.W., Acevedo, C., Benavides, U., Seixas, A., Logullo, C., Konnai, S., Ohashi, K., Masuda, A., Vaz, da Silva, I, Jr, 2013. Sequence characterization and immunogenicity of cystatins from the cattle tick *Rhipicephalus (Boophilus) microplus*. Ticks Tick Borne Dis. 4, 492–499.

Parizi, L.F., Sabadin, G.A., Alzugaray, M.F., Seixas, A., Logullo, C., Konnai, S., Ohashi, K., Masuda, A., Vaz, da Silva, I, Jr, 2015. *Rhipicephalus microplus* and *Ixodes ovatus* cystatins in tick blood digestion and evasion of host immune response. Parasit. Vectors 8, 122.

Parizi, L.F., Rangel, C.K., Sabadin, G.A., Saggin, B.F., Kiio, I., Xavier, M.A., Matos, R.D., Camargo-Mathias, M.I., Seixas, A., Konnai, S., Ohashi, K., Githaka, N.W., Vaz, I.D., 2020. *Rhipicephalus microplus* cystatin as a potential cross-protective tick vaccine against *Rhipicephalus appendiculatus*. Ticks Tick-Borne Dis. 11.

Perner, J., Provaznik, J., Schrenkova, J., Urbanova, V., Ribeiro, J.M., Kopacek, P., 2016a. RNA-seq analyses of the midgut from blood- and serum-fed *Ixodes ricinus* ticks. Sci. Rep. 6, 36695.

Perner, J., Sobotka, R., Sima, R., Konvickova, J., Sojka, D., de Oliveira, P.L., Hajdusek, O., Kopacek, P., 2016b. Acquisition of exogenous haem is essential for tick reproduction. eLife 5.

Pipano, E., Alekceev, E., Galker, F., Fish, L., Samish, M., Shkap, V., 2003. Immunity against *Boophilus annulatus* induced by the Bm86 (Tick-GARD) vaccine. Exp. Appl. Acarol. 29, 141–149.

Rachinsky, A., Guerrero, F.D., Scoles, G.A., 2008. Proteomic profiling of *Rhipicephalus (Boophilus) microplus* midgut responses to infection with *Babesia bovis*. Vet. Parasitol. 152, 294–313.

Rand, K.N., Moore, T., Sriskantha, A., Spring, K., Tellam, R., Willadsen, P., Cobon, G.S., 1989. Cloning and expression of a protective antigen from the cattle tick *Boophilus microplus*. Proc. Natl. Acad. Sci. U. S. A. 86, 9657–9661.

Reck, J., Berger, M., Terra, R.M.S., Marks, F.S., Vaz, I.D., Guimaraes, J.A., Termignoni, C., 2009. Systemic alterations of bovine hemostasis due to *Rhipicephalus (Boophilus) microplus* infestation. Res. Vet. Sci. 86, 56–62.

Rego, R.O.M., Trentelman, J.J.A., Anguita, J., Nijhof, A.M., Sprong, H., Klempa, B., Hajdusek, O., Tomas-Cortazar, J., Azagi, T., Strnad, M., Knorr, S., Sima, R., Jalovecka, M., Havlikova, S.F., Lickova, M., Slavikova, M., Kopacek, P., Grubhoffer, L., Hovius, J.W., 2019. Counterattacking the tick bite: towards a rational design of anti-tick vaccines targeting pathogen transmission. Paras. Vector 12.

Reyes, J., Ayala-Chavez, C., Sharma, A., Pham, M., Nuss, A.B., Gulia-Nuss, M., 2020. Blood digestion by trypsin-like serine proteases in the replete lyme disease vector tick. *Ixodes scapularis. Insects* 11.

Ribeiro, J.M.C., Mans, B., 2020. TickSialoFam (TSFam): a database that helps to classify tick salivary proteins, a review on tick salivary protein function and evolution, with considerations on the tick sialome switching phenomenon. Front. Cell Infect. Mi 10.

Roberts, J.A., 1968. Resistance of cattle to the tick *boophilus microplus* (canestrini). I. Development of ticks on Bos taurus. J. Parasitol. 54, 663–666.

Robinson, M.D., McCarthy, D.J., Smyth, G.K., 2010. edgeR: a Bioconductor package for differential expression analysis of digital gene expression data. Bioinformatics 26, 139–140.

Schwarz, A., Tenzer, S., Hackenberg, M., Erhart, J., Gerhold-Ay, A., Mazur, J., Kuharev, J., Ribeiro, J.M., Kotsyfakis, M., 2014. A systems level analysis reveals transcriptomic and proteomic complexity in *Ixodes ricinus* midgut and salivary glands during early attachment and feeding. Mol. Cell. Proteomics 13, 2725–2735.

Seixas, A., Alzugaray, M.F., Tirloni, L., Parizi, L.F., Pinto, A.F.M., Githaka, N.W., Konnai, S., Ohashi, K., Yates, J.R., Termignoni, C., Vaz, I.D., 2018. Expression profile of *Rhipicephalus microplus* vitellogenin receptor during oogenesis. Ticks Tick-Borne Dis. 9, 72–81.

Shahein, Y.E., El-Hakim, A.E.S., Abouelella, A.M.K., Hamed, R.R., Allam, S.A.M., Farid, N.M., 2008. Molecular cloning, expression and characterization of a functional GSTmu class from the cattle tick *Boophilus annulatus*. Vet. Parasitol. 152, 116–126.

Shamir, R., Maron-Katz, A., Tanay, A., Linhart, C., Steinfeld, I., Sharan, R., Shiloh, Y., Elkon, R., 2005. EXPANDER–an integrative program suite for microarray data analysis. BMC Bioinformat. 6, 232.

Silva, F.D., Rezende, C.A., Rossi, D.C.P., Esteves, E., Dyszy, F.H., Schreier, S., Gueiros-Filho, F., Campos, C.B., Pires, J.R., Daffre, S., 2009. Structure and mode of action of microplusin, a copper ii-chelating antimicrobial peptide from the cattle tick *Rhipicephalus (Boophilus) microplus*. J. Biol. Chem. 284, 34735–34746.

Simao, F.A., Waterhouse, R.M., Ioannidis, P., Kriventseva, E.V., Zdobnov, E.M., 2015. BUSCO: assessing genome assembly and annotation completeness with single-copy orthologs. Bioinformatics 31, 3210–3212.

Simpson, J.T., Wong, K., Jackman, S.D., Schein, J.E., Jones, S.J., Birol, I., 2009. ABySS: a parallel assembler for short read sequence data. Genome Res. 19, 1117–1123.

Soares, T.S., Watanabe, R.M., Tanaka-Azevedo, A.M., Torquato, R.J., Lu, S., Figueiredo, A.C., Pereira, P.J., Tanaka, A.S., 2012. Expression and functional characterization of boophilin, a thrombin inhibitor from *Rhipicephalus (Boophilus) microplus* midgut. Vet. Parasitol. 187, 521–528.

Sonenshine, D.E., Roe, R.M., 2013. Biology of Ticks. Oxford University Press, 2 ed.

Stutzer, C., van Zyl, W.A., Olivier, N.A., Richards, S., Maritz-Olivier, C., 2013. Gene expression profiling of adult female tissues in feeding *Rhipicephalus microplus* cattle ticks. Int. J. Parasitol. 43, 541–554.

Team, R.C. (2020) R: a Language and Environment for Statistical Computing.

Tirloni, L., Lu, S., Calvo, E., Sabadin, G., Di Maggio, L.S., Suzuki, M., Nardone, G., Vaz, I. D., Ribeiro, J.M.C., 2020a. Integrated analysis of sialotranscriptome and sialoproteome of the brown dog tick *Rhipicephalus sanguineus* (s.l.): insights into gene expression during blood feeding. J. Proteomics 229.

Jr. Tirloni, L., Braz, G., Nunes, R.D., Gandara, A.C.P., Vieira, L.R., Assumpcao, T.C., Sabadin, G.A., Silva, da, R, M., Guizzo, M.G., Machado, J.A., Costa, E.P., Santos, D., Gomes, H.F., Moraes, J., Mota, Dos Santos, M, B., Mesquita, R.D., de Souza Leite, M., Alvarenga, P.H., Lara, F.A., Seixas, A., Fonseca, da, R, N., Fogaca, A.C., Logullo, C., Tanaka, A.S., Daffre, S., Oliveira, P.L., da Silva, Vaz, I., Ribeiro, J.M.C, 2020b. A physiologic overview of the organ-specific transcriptome of the cattle tick *Rhipicephalus microplus* Sci. Rep. 10, 18296.

Umemiya-Shirafuji, R., Mihara, R., Fujisaki, K., Suzuki, H., 2019. Intracellular localization of vitellogenin receptor mRNA and protein during oogenesis of a parthenogenetic tick, *Haemaphysalis longicornis*. Parasite Vector 12.

Wei, N., Du, Y., Lu, J., Zhou, Y., Cao, J., Zhang, H., Gong, H., Zhou, J., 2020. A cysteine protease of *Babesia microti* and its interaction with tick cystatins. Parasitol. Res. 119, 3013–3022.

Willadsen, P., Riding, G.A., McKenna, R.V., Kemp, D.H., Tellam, R.L., Nielsen, J.N., Lahnstein, J., Cobon, G.S., Gough, J.M., 1989. Immunologic control of a parasitic arthropod. Identification of a protective antigen from *Boophilus microplus*. J. Immunol. 143, 1346–1351.

Yang, X.L., Koci, J., Smith, A.A., Zhuang, X.R., Sharma, K., Dutta, S., Rana, V.S., Kitsou, C., Yas, O.B., Mongodin, E.F., Pal, U., 2021. A novel tick protein supports integrity of gut peritrophic matrix impacting existence of gut microbiome and Lyme disease pathogens. Cell. Microbiol. 23.